Mineral weathering and lessivage affect microbial community and enzyme activity in mountain soils

MINERAL WEATHERING AND LESSIVAGE AFFECT MICROBIAL COMMUNITY AND ENZYME ACTIVITY IN MOUNTAIN SOILS

Marinari S.[a]*, Marabottini, R. [a], Falsone G.[b], Vianello G.[b], Vittori Antisari L.[b], Agnelli A.[c,e], Massaccesi L.[c], Cocco S.[d], Cardelli V.[d], Serrani D.[d], Corti G.[d]

[a]Dipartimento per l'Innovazione nei sistemi Biologici, Forestali e Agroalimentari, Università degli Studi della Tuscia, Italy

[b]Dipartimento di Scienze e Tecnologie Agro-Alimentari, Alma Mater Studiorum Università di Bologna, Italy

[c] Dipartimento di Scienze Agrarie, Alimentari e Ambientali, Università degli Studi di Perugia, Italy

[d] Dipartimento di Scienze Agrarie, Alimentari ed Ambientali, Università Politecnica delle Marche, Ancona, Italy

[e] Research Institute on Terrestrial Ecosystem (IRET-CNR), Italy

***Corresponding author: marinari@unitus.it**

Abstract

The aim of the study was to assess if pedogenic processes such as mineral weathering and lessivage, other than organic matter accumulation, can affect soil microbial population and enzyme activities. This study examines six soil profiles located in a karst region of the North-Eastern Italian Alps and characterized by a vertical textural differentiation due to lessivage. For each soil, four pedological layers were recognized according to the dominant soil forming process: *i*) the top soil (Tp layer), formed by A and AB horizons, characterized by organic matter accumulation; *ii*) the subsurface eluviated layer (Elu layer), comprising AE and EB horizons; *iii*) the layer dominated by the in-situ mineral weathering (Wh layer), made by Bw horizons; *iv*) the deepest layer (Ls), subjected to clay illuviation and comprised by Bt horizons. In the upper layers (Tp and Elu), because of the low pH, weathering also occurred, as indicated by the presence of disordered smectite and by the high values of pedogenic Fe oxi-hydroxides to pseudo-total Fe ratio.

The microbial biomass content and structure, and the enzyme activities significantly differed in the four pedological layers. The amount of microbial biomass was, as expected, most abundant in the Tp layer, where bacteria and actinomycetes abounded. Conversely, in Elu and Wh we observed a fungal-to-bacterial biomass ratio significantly higher than in Tp and Ls; in Elu, also the gram (+)/ gram (-) ratio was the highest. In the upper layer, the interaction between enzymes and minerals like disordered smectite and pedogenic Fe-oxides appeared as responsible for the inhibition of the total enzyme activity per unit of organic C, and of the lipase activity. In Ls layer, where clay illuviation and high organo-minerals interaction occurred, the potential hydrolysis of organic matter was low, as revealed by the SEI/TOC ratio, the reduced lipase activity, and the inhibited activity of α-fucosidase and α-mannosidase. Even if the activity of most enzymes depends on the substrate availability, which decreases with soil depth, those involved in lipid degradation displayed the maximum activities in Elu and Wh layers, where a relative increase of the fungal population was observed. In conclusion, our findings showed that the soil functionality, expressed by the microbial

community structure and enzymes activity, can vary according to organic matter–mineral interaction following the weathering and lessivage gradients along the soil profiles.

Keywords: pedogenic processes, microbial biomass, organo-mineral interactions, illuviation, soil horizons.

1. Introduction

Mountain soils are often weakly developed because of several limiting factors such as steep slope and low temperature, which accelerate soil erosion and slow down the mineral weathering and organic matter oxidative kinetics, respectively (Legros, 1992; De Feudis et al., 2019; Cardelli et al., 2019; Massaccesi et al., 2020). Among the soil forming processes occurring in mountain soils, organic matter accumulation at soil surface (e.g., Boča and Miegroet, 2017), decomposition/neoformation of clay minerals, and translocation of clay particles and organics along the soil profile (Bockheim and Gennadiyev, 2000) are frequent. The organic and mineral phases can reciprocally affect themselves, with soil organic matter (SOM) enhancing mineral weathering and controlling the formation of secondary minerals (e.g., Anderson et al., 1982; Dahlgren and Ugolini, 1989), which in turn contribute to SOM stabilization (e.g., Eusterhues et al., 2003). The organo-mineral interactions are one of the main mechanisms driving the stabilization of SOM, and the nature of clay minerals controls this process (e.g., Mikutta et al., 2007; Agnelli et al., 2008; Kögel-Knabner et al., 2008; Barré et al., 2014; Gartzia-Bengoetxea et al., 2020). The ability of clay minerals to stabilize SOM is function of the reactivity of the mineral surfaces (e.g., Mikutta et al., 2006; Wang et al., 2017), which decreases from high-charge phyllosilicates such as vermiculites and smectites to illite and kaolinite (Bruun et al., 2010). As a part of SOM, also enzymes can be stabilized by clay minerals, either by adsorption through enzyme active-sites and occlusion in micro-aggregates (Sollins et al., 1996). These mechanisms limit the substrate accessibility and contribute to form a reservoir of potential enzymatic activity into the soil (Burns et al., 2013) by protecting enzymes against proteolysis and denaturation (Nannipieri et al., 2012). Because of this, the enzyme activity is considered a sensitive indicator of ecotoxicological pollution (Turan, 2019; Bilen et al., 2019). The ecological benefit of the organo-mineral interactions including enzymes has demonstrated to play a key role also in terms of soil resilience (Benitez et al., 2004).

In soils affected by lessivage, clay minerals and their colloidal properties can further control *i*) the possible translocation of the organo-mineral complexes, and *ii*) the formation of eluviated and illuviated horizons (E and Bt, respectively) due to mobilisation, transport, and deposition of clay particles or clay-humus complexes within the soil profile (Schaetzl and Anderson, 2005). Furthermore, decomposition and synthesis of clay minerals are two processes often associated with lessivage (Presley et al., 2004; Schaetzl and Anderson, 2005). Clay and clay minerals can be weathered in the upper and more acidic soil compartment by congruent dissolution and the soluble by-products translocated in the B horizons, where they precipitate to form new minerals (Shaetzl and Anderson, 2005). When the lessivage is dominant on mineral weathering, the clay mineralogical assemblage in the eluviated and illuviated horizons is usually similar, whereas under decomposition/neoformation processes the clay mineralogy can be strongly different. Consequently, organo-mineral interaction, and thus microbial biomass and enzyme activities, can be affected by the amount and nature of clay minerals (Torn et al., 1997; Wiseman and Püttmann, 2005; Mikutta et al., 2006),

Since, as far as we know, few papers focused on the effects of pedogenic processes on soil biochemical properties (e.g., Vittori Antisari et al., 2018), a combined pedological, chemical, and biochemical approach has been adopted in this study to increase the knowledge on the soil microbial community and enzymatic activity along the pedon. Specifically, the aim of this work was to assess if lessivage and/or mineral weathering, other than SOM accumulation, can influence microbial community structure and enzyme activity in mountain soils. We hypothesized that, although SOM accumulation is the main driver of the soil biochemical activity, lessivage and mineral weathering could act as limiting factors for the enzyme activities involved in the nutrient cycling through organo-mineral interactions. We tested the hypothesis by a physicochemical, mineralogical, and biochemical approach on six soil profiles with evident vertical textural differentiation due to lessivage in a karst region located in the North-Eastern Italian Alps.

2. Materials and Methods

2.1 Study area and soil sampling

The study area was located close to the Brocon Pass (1600 m above sea level), North-eastern Italian Alps (Figure 1), where the soils developed on the so called "scaglia rossa", a thinly-layered, red to reddish-pink marly limestone interbedded with clayey micritic limestones and shales (Tosoni, 2011). This rock has variables contents of clay minerals like micas and smectites (ISPRA, 2010), and the colour is due the dispersion of iron oxides (mainly hematite and goethite) in the limestone mass (Bertola and Cusinato, 2004).

The area is characterized by moderate to steep slopes covered by herbaceous vegetation mainly composed of *Festuca paniculata* (L.) Schinz & Thell. subsp. *paniculata* and *Cirsium eriophorum* L. (Table S1), and it is intensively pastured during the summer-autumn period. The climate is continental with cold winters and hot summers. The mean annual air temperature is 4.4 °C, with July as the warmest month (15.7 °C) and December as the coldest one (-2.7 °C). The mean annual precipitation, including the snow water equivalent, is 976 mm. The soil is covered by snow from mid-October till the end of April.

Six sites were selected within an area of about 0.55 ha (Figure 1). For each site, a soil profile was dug to investigate the solum and the relationship between the soil forming processes and the physicochemical and biochemical soil properties. All the profiles were described by Schoeneberger et al. (2012) (Table S1). The investigated soils had a depth that varied from 37 to 60 cm (Table S1), with the topsoil characterized by well-developed O horizons (1.5-4 cm thick) resting on A, AB, or AE horizons (9-21 cm thick); below the topsoil, rather thick Bw and Bt horizons formed. Even if the soils developed from calcareous parent materials, during the field operations the soil material never showed effervescence with 10% HCl solution, indicating the absence of $CaCO_3$ in the solum. This feature testified the occurrence of decarbonation along the investigated soil thickness.

Soil samples were collected by genetic horizons and maintain in a refrigerated bag for all the field operations. Once in the laboratory, ¾ of each soil sample were air dried and sieved at 2 mm, while the rest was kept at 4 °C for the biochemical analyses.

2.2 Soil physical and chemical analyses

The particle-size distribution was determined by the pipette method (Gee and Bauder, 1986) after treatment with NaClO solution at 6% of active chlorine to remove organic cements (Lavkulich and Wiens, 1970) and with dithionite-citrate-bicarbonate solution to remove Fe-Al oxi-hydroxides cements (Mehra and Jackson, 1960). The clay fraction was collected for the mineralogical analysis. The pH was determined potentiometrically in water after one night of solid:liquid (1:2.5 w:v ratio) contact, using a combined glass-calomel electrode immersed into the suspension. The electrical conductivity (EC) was determined by a WTW multi 340i conductivity meter (Weilheim, Germany) in a 1:2.5 soil:water suspensions (w:v). Total organic carbon (TOC) and total nitrogen (TN) were measured using the dry combustion method with Thermo Soil NC—Flash EA1112 elemental analyser. The exchangeable cations were displaced by hexamine cobalt (III) chloride (Orsini and Remy, 1976). The displaced Ca, Mg, K, Na, and Al were determined by Inductive Coupled Plasma – Optic Emission Spectroscopy (ICP-OES, Ametek Germany). Exchangeable H was calculated as the pH difference between the 0.2 M $BaCl_2$ solution before and after contact with the soil samples (Corti et al., 2019). Effective cation exchange capacity (eCEC) was obtained as the summation of all exchangeable cations (Ca, Mg, K, Na, Al, and H). The base saturation was obtained by dividing the sum of exchangeable Ca, Mg, K, and Na by the eCEC value.

Pedogenic Fe and Al oxi-hydroxides were measured through extraction with Na-dithionite-citrate-bicarbonate solution (Fe_{DCB} and Al_{DCB}) (Mehra and Jackson, 1960). Fe and Al in the extracts were measured by ICP-OES. The pseudo-total amount of Al, Fe, Ca, Mg, K, Na, Mn, P and S (Al_T, Fe_T, Ca_T, Mg_T, K_T, Na_T, Mn_T, P_T, and S_T) was obtained digesting finely ground sample aliquots in polyethylene vials with *aqua regia* (3:1 HCl:HNO_3) in microwave oven (Milestone, 1200)

150 according to Vittori Antisari et al. (2014); then, the concentration of each element in the extract was
151 measured by ICP-OES. The Fe_{DCB}/Fe_T ratio was taken as an index of the amount of pedogenic Fe-
152 oxides with respect to the total Fe (Fe_T) (Qafoku and Amonette, 2017). The ratio between the molar
153 sum of Ca_T, Mg_T, K_T, and Na_T and the molar sum of Al_T and Fe_T [$(Ca_T+Mg_T+K_T+Na_T)/(Al_T+Fe_T)$],
154 which represent the most and less mobile groups of elements, respectively (Chadwick et al., 1999),
155 was calculated to assess the redistribution of the elements along soil profile driven by their mobility.
156
157 *2.3 Mineralogical analysis*
158 Mineralogical assemblage was determined on powdered and manually compressed aliquots by X-
159 ray diffraction with a Philips PW 1830 diffractometer, using the Fe-filtered Co Kα1 radiation (35
160 kV and 25 mA); the step size was 0.02°2θ, the scanning speed was 1 sec per step, and sample
161 aliquots were scanned from 3 to 80°2θ. The mineralogical composition was obtained by identifying
162 the minerals based on their characteristic peaks (Brindley and Brown, 1980; Dixon and Schulze,
163 2002). For each sample, a semi-quantitative estimation was obtained by calculating the area
164 produced by the primary peak of each mineral by multiplying the peak height by the base at the
165 half-height. The clay fraction was Mg- or K-saturated; the Mg-saturated clays were
166 glycerol solvated, while the K-saturated ones were heated at 550 °C. The presence of Al-
167 hydroxopolymers in the interlayers of the 2:1 clay minerals was ascertained, and their thermo-
168 stability assessed, by K-saturated and heated at 550 °C specimens (Brindley and Brown, 1980; Corti
169 et al., 1997; Dixon and Schulze, 2002).
170
171 *2.4 Soil biochemical analysis*
172 Soil microbial biomass C (MBC) and N (MBN) were determined using the fumigation-extraction
173 method (Brookes et al., 1985; Vance et al., 1987). MBC was obtained by $eC \cdot k_{eC,}$ where eC was the
174 difference between organic C extracted using 0.5 M K_2SO_4 solution (1:4 w/v) from fumigated and

not-fumigated samples, and $k_{eC} = 2.64$ is the extraction efficiency coefficient (Joergensen, 1996). The amount of C extracted by K_2SO_4 solution from non-fumigated samples (C_{ext}) was considered the easily extractable and most labile soil organic C pool. MBN was calculated by $eN \cdot k_{eN}$, where eN is the difference between N extracted using 0.5 M K_2SO_4 solution (1:4 w/v) from fumigated and not-fumigated samples and $k_{eN} = 2.22$ is the extraction efficiency coefficient (Jenkinson, 1988). The extracted C and N were determined with the TOC-V CSN and TNM-1 analysers (Shimadzu, Japan). The living microbial biomass was determined as the sum of all microbial groups obtained using Ester linked-Fatty Acid Methyl Ester (El-FAME). The microbial community profiles were determined, quantified, and converted to $\mu mol \cdot g^{-1}$ using peak areas from internal standard (methylnonadecanoate, C19:0) used at known concentrations. A total of 13 El-FAME biomarkers were summed into the broad microbial groups Actinobacteria (10Me16,0, 10Me17:0, 10Me18:0), Gram-positive (G+) bacteria (i15:0, a15:0, i16:0, i17:0, a17:0), Gram-negative (G-) bacteria (cy 17:0, cy 19:0ω8c, 18:1 ω7c), and saprophytic fungi (18,1 ω9c, 18:2 ω6c), according to previous studies (Zelles, 1999; Massaccesi et al., 2015; Stazi et al., 2017). The per mil fungal-to-bacteria ratio (F/B) was calculated as an index of soil microbial community change, while G+/G- ratio was proposed as an indicator of stressful conditions such as low oxygen availability, suboptimal pH or water content, or low nutrient supply because of the greater dependence of G- than G+ on labile C (Fanin et al., 2019). Moreover, the sum of El-FAMEs characteristic of general bacteria, G+ and G− bacteria, actinomycetes, and fungi was used as broad taxonomic microbial grouping.

The soil enzyme activities were measured using 4-methylumbelliferine (MUF) and 7-amino-4-methylcoumarin (AMC) fluorogenic substrates (Marx et al., 2001; Vepsäläinen et al., 2001). The selected 17 enzyme activities (Table S2) are involved in the main biogeochemical cycle of C (β-cellobiohydrolase, β–xylosidase, β-glucosidase, α-glucosidase, α-galactosidase, β-galactosidase, β-glucuronidase, α-mannosidase, α-fucosidase, butyrate esterase, esterase lipase, and lipase activities), N (leucine-arylamidase, valine arylamidase, and N-acetyl-β-glucosaminidase activities), P (acid phosphomonoesterase activity), and S (arylsulphatase activity). Even if the pH values of the studied

soil samples ranged from 4.3 to 6.9, enzymes involved in a wide range of substance degradation with optimal pH in acid and alkaline intervals were selected (Table S2). Therefore, specific substrates were prepared using different buffer adjusted to the optimum for each selected enzyme (0.5 M sodium acetate pH 5.5; 0.5 M Tris acetate pH 7.5). Fluorescence (excitation 360 nm, emission 450 nm) was measured with an automatic fluorometric plate reader (Fluoroskan Ascent), and readings were performed after 0, 30, 60, 120, and 180 min at 30 °C. The MUF and the AMC standard curves were prepared and measured for each sample and buffer. The results were expressed as nmoles of product (MUF or AMC) of each enzymatic reaction released per g of soil sample per unit of time in relation to a standard curve prepared with increasing MUF or AMC concentrations and incubated at the same experimental conditions. The Synthetic Enzymatic Index (SEI), which expresses the sum of all enzyme activities, was calculated for all samples as a synthetic measure of microbial functional capacity (Moscatelli et al., 2018). Based on the obtained data, the specific enzyme activities per unit of TOC (SEI/TOC) was calculated to appraise the nutritional status of SOM (Boerner et al., 2005; Trasar-Cepeda et al., 2008).

2.5 Data treatment

In the studied soils, four pedological layers were recognized according to the dominant soil forming process: *i*) the topsoil layer (Tp), characterized by SOM accumulation and comprising the A and AB horizons; *ii*) the sub-surface layer (Elu), providing indication of past or on going eluvial processes and made of AE and EB horizons; *iii*) the intermediate portion of the soil profile (Wh), characterized by *in-situ* mineral weathering and represented by Bw horizons; *iv*) the deepest layer (Ls), subjected to clay illuviation and formed by Bt horizons. For each layer (Tp, Elu, Wh, and Ls), the physicochemical, mineralogical, and biochemical properties have been calculated as the average of the corresponding horizons for the six soil profiles. Because of the non-parametricity of the data and the impossibility to transform them into parametrically distributed data, the significant

differences among the layers were checked by using the non-parametric Wilcoxon test. To define the soil properties driving the layers differentiation, a principal component analysis (PCA) was run for both physicochemical and biochemical data obtained from 30 soil samples (one per each horizon) collected from the six profiles. This multivariate analysis is based on the linear model of variance analysis and consists of decomposing the total variability among soil properties. The variables were standardized due to the difference in the units of measure. The applicability of the PCA to the data sets was verified through the application of Bartlett's sphericity test. Non-parametric correlation (Spearman coefficient) was performed between physicochemical and biochemical soil properties. Statistical analysis was performed using JMP 11.0 software.

3. Results

3.1 Soil physicochemical characteristics

The pH values of Tp, Elu, and Wh layers were strongly acid, with average values ranging from 4.55 to 4.82, while the deepest layer (Ls) significantly differed, reaching a moderately acid pH value of 5.97 (Table 1). The TOC and TN contents significantly decreased with depth (Table 1) and the same trend was observed for P_T and S_T contents (Table 1). The C_{extr} concentration (Table 1), which represented 1.80-3.43% of TOC, showed a decreasing trend with depth. Conversely, the concentrations of Al_T, Fe_T, Ca_T, Mg_T, and K_T increased with depth (Table 2), while Mn_T and Na_T had a homogenous content all throughout the profiles. The total clay content increased along the profiles (Table 2), with the highest values, as expected, in Ls (692 g kg^{-1}). The eCEC values were similar among soil layers (from 29.0 to 31.1 $cmol_+$ kg^{-1}) and the base saturation was always higher than 50%. The EC values were lower in Elu and Wh (on average 0.07 and 0.09 dS m^{-1}, respectively) than in Tp and Ls (0.35 and 0.20 dS m^{-1}). The content of pedogenic Fe and Al (Fe_{DCB} and Al_{DCB}) did not displayed a linear trend with depth (Table 2), but the Fe_{DCB}/Fe_T ratio (Figure 2A) had the highest values ($p<0.01$) in Tp and Elu horizons (0.65 and 0.72, respectively). The

251 (Ca_T+Mg_T+K_T+Na_T)/(Al_T+Fe_T) molar ratio showed lower values ($p<0.01$) in Tp, Elu, and Wh than
252 in Ls (Figure 2B). For these physicochemical data, the PCA has allowed to extract two principal
253 components with eigenvalues greater than 2 (Figure 3). The two-component model accounted for
254 64.5% of the total variance, with the first and the second axes explaining 41.6% and 22.9% of total
255 variation, respectively. The Table inserted in Figure 3 indicates that the first axis showed high
256 positive loadings for TOC, TN, P_T, S_T, and Fe_{DCB}/Fe_T ratio and high negative loading for C_{extr}/TOC
257 ratio. The second axis was positively driven by pH, EC, (Ca_T+Mg_T+K_T+Na_T)/(Al_T+Fe_T) molar
258 ratio, and total clay. The PCA highlighted some differences among the four layers: *i*) Tp layer
259 generally showed positive values of both components; *ii*) Elu layer displayed positive values for the
260 first component and negative values for the second one; *iii*) Wh layer exhibited negative values for
261 both components; *iv*) Ls layer presented negative values for the first component and positive values
262 for the second one (Figure 3).
263
264 *3.2 Soil mineralogy*
265 The semi-quantitative mineralogical composition showed that quartz was the predominant primary
266 mineral (from 41 to 47%), with plagioclases, orthoclase, and micas present in small amounts (Table
267 3). All the samples showed the presence of a peak at 1.4 nm that moved to ≈1.8 nm after glycerol
268 solvation, and partially collapsed at ≈1.0 nm when the K-saturated specimen was heated at 550 °C,
269 indicating the presence of smectite (Figure S1). The 1.0 nm peak in the heated specimens was
270 however rather wide and asymmetrical in all samples, with the exception for those of the horizons
271 forming the Elu layers. A peak at 0.7 nm was detected in the Mg-saturated specimens and
272 disappeared after heating at 550 °C, indicating the presence of kaolinite. Therefore, in all the
273 horizons, the clay minerals were mainly represented by smectite (from 31 to 35%) and kaolinite
274 (from 2 to 5%). Smectite was also present as disordered layer minerals, as deduced from the broad
275 diffraction band between 1.4 and 1.5 nm of the Mg-saturated specimens and between 1.8 and 1.95

276 nm in the Mg-saturated and glycerol-solvated specimens. The pronounced asymmetry of the 1.0 nm
277 peak after specimen heating was indicative of Al polymers in the smectite interlayers, which
278 prevented the complete collapse of smectite at 550 °C (Table 3). In particular, disordered smectite
279 was present in the Tp and Elu layers, whereas HIS were absent in Elu layer.
280
281 *3.3 Microbial biomass and enzyme activities*
282 The amounts of MBC and MBN were significantly higher ($p<0.05$; Table 4) in Tp (874 and 246 mg
283 kg^{-1}, respectively) than in the deeper soil layers (Wh and Ls; 118 and 227 mg MBC kg^{-1}; 45 and 81
284 mg MBN kg^{-1}), while Elu layer displayed intermediate amounts (445 and 151 mg kg^{-1},
285 respectively). Conversely, the amount of the living microbial biomass expressed as the sum of the
286 microbial groups assessed by El-FAME and of bacteria and actinomycetes were the highest in Tp
287 (464, 449, and 53.5 nmol g^{-1}, respectively) and the lowest in Elu (63, 59, and 6.8 nmol g^{-1},
288 respectively). Furthermore, the F/B ratio was greater in Elu and Wh (47.5 and 39.1‰, respectively)
289 than in Tp and Ls (28.2 and 24.4‰), while the G+/G- ratio displayed the highest value in Elu (1.02)
290 (Table 4).
291 The enzyme activities involved in the C cycle (β-cellobiohydrolase, α- and β-glucosidase, β–
292 xylosidase, β-galactosidase, and β-glucuronidase) were the highest in Tp (76.3, 79, 389, 189, 89,
293 and 203 nmol MUF g^{-1} h^{-1}, respectively), and showed a significant reduction of their activity
294 starting from Elu (Table 5). Conversely, enzymes involved in N, P, and S cycles (N-acetyl-ß-
295 glucosaminidase, leucine arylamidase, butyrate esterase, acid phosphomonoesterase, and
296 arylsulphatase) showed the highest activities in Tp and Elu layers and significantly decreased in Wh
297 or Ls (Table 5). Two over 17 enzyme activities, esterase lipase and valine arylamidase, did not
298 show any significantly change along the profiles, whereas α-mannosidase and α-fucosidase showed
299 a very low activity in Ls (9.7 and 8.2 nmol MUF g^{-1} h^{-1}, respectively; Figure 4A and B).
300 Conversely, the lipase had the lowest activity in Tp and Ls (154 and 197 nmol MUF g^{-1} h^{-1},

301 respectively) and the highest in Wh (359 nmol MUF g^{-1} h^{-1}; Figure 5A). The total enzyme activity
302 expressed per unit of organic carbon (SEI/TOC) displayed a similar trend of lipase (Figure 5B),
303 reaching in Ls an average value similar to that of Tp (110 *vs*. 77 nmol MUF mg_{TOC}^{-1} h^{-1};
304 respectively).
305 Compared to the others, lipase and esterase lipase activities were not correlated with pH, TOC, TN,
306 C_{extr}/TOC, clay content, and Fe_{DCB}/Fe_T (Table 6); lipase activity only showed negative correlations
307 with electrical conductivity (EC) and $(Ca_T+Mg_T+K_T+Na_T)/(Al_T+Fe_T)$ ratio. The PCA run with the
308 soil biochemical data showed that 10 over the 17 enzyme activities had positive loading values
309 along the first component, which explained 62.8% of the total variance (Figure 6). Conversely, the
310 other seven enzyme activities (α-mannosidase, α-fucosidase, butyrate esterase, esterase lipase,
311 α−galactosidase, β-galactosidase, and lipase) were mainly correlated with the second component,
312 explaining 14.1% of the total variance.
313

314 **4. Discussion**

315 The clay coatings on soil peds observed in the profiles (Table S1) and the increasing amount of clay
316 particles with depth (Table 2) proved that clay illuviation occurred in these soils and that this
317 process was responsible for the formation of Bt (illuviated) horizons. It is well known that clay
318 eluviation (with the formation of eluviated horizons) occurs mainly at pH values ranging between
319 4.5/5 and 6; below this range clay flocculates because of a high Al^{3+} and H^+ activity in the soil
320 solution, while at higher pHs clay flocculates because of a high concentration of Ca^{2+} or other
321 divalent cations in the soil solution (Quénard et al., 2011). Accordingly, in the acid horizons (pH
322 4.55-4.82) of our soils clay eluviation could occurred, whereas in the deep Ls layer the slight
323 increase of soil reaction (pH 5.97) induced clay to flocculate so to form illuviated horizons. In Ls,
324 the clay flocculation was possibly enhanced by the leached soluble elements (Levy et al., 1993;

Kaplan et al., 1997), which were able to increase the EC values with respect to the overlying Elu and Wh layers.

The similar mineralogical assemblage of the four layers supported the occurrence of lessivage and suggested that clay decomposition/neoformation processes along the soil profiles were limited. The presence of small amounts of hydroxy-Al interlayered smectite (HIS) indicated that weathering has occurred through the intercalation of hydroxy-Al polymers into the smectite interlayers. This transformation is rather common in soil affected by lessivage (e.g., Bonifacio et al., 2009). In particular, the large presence of disordered smectite and very small amounts of HIS in the Elu layer indicated the occurrence of weathering processes promoted by low pH values and of accumulation of organic matter in the upper part of the soil profiles, as reported in several works carried out on Italian mountains soils (e.g., Vittori Antisari et al., 2016; De Feudis et al., 2016; 2017a, b; Cardelli et al., 2019). The occurrence of mineral weathering in Elu, as well as in Tp, is also confirmed by the relatively high Fe_{DCB}/Fe_T ratio and by the PCA on soil physicochemical properties, which grouped Tp and Elu layers into two well distinguished ellipses with respect to Wh and Ls (Figure 3).

The soil microbial biomass and the total enzyme activity (SEI) decreased with soil depth. These results are usually found in soil since both these parameters largely depend on the amount and quality of soil organic matter (Fierer et al., 2003; Sidari et al., 2008; Agnelli et al., 2016). However, according to the PCA loading values on the first two PCs (Figure 6), soil biochemical properties mainly depended on SOM accumulation process in Tp and Elu layers. Therefore, the highest values of TOC content, coupled with the accumulation of N, P, and S in Tp and Elu, favoured the soil microbial community (Likens et al., 2002; De Feudis et al., 2016; Adams et al., 2018), as indicated by the higher MBC and SEI. Nonetheless, other processes than SOM accumulation affected the biochemical properties of the investigated soils. Indeed, while TOC, TN, P_T, and S_T contents did not significantly differ between Wh and Ls, SEI differed between them. As the main pedogenic process at depth was the formation of Bt horizons due to clay illuviation, the lower SEI in Ls than in Wh was ascribed to a higher inhibition of the enzyme activity due to the sorption of organics (including

enzymes) onto clay minerals (Singh et al., 2018), as demonstrated by the significant negative correlation between SEI and clay content. By expressing the enzyme activity per unit of organic carbon (SEI/TOC), it was possible to stress the effect of both lessivage and weathering processes (Marinari et al., 2020). In Ls, the hydrolytic activity per unit of TOC was lower than in Wh, probably due to the organo-mineral interactions among substrates, enzymes, and the illuviated clay. However, the SEI/TOC ratio was low also in Tp, where SOM accumulation was coupled to relatively intense weathering conditions, as testified by the presence of disordered smectite and a relatively high Fe_{DCB}/Fe_T ratio. According to Singh et al. (2018), in the Tp layer a strong inhibition of the enzyme activities (per unit of TOC) probably occurred because of the interactions between enzymes and smectite and/or pedogenic oxides.

A specific behaviour was observed for enzyme activities involved in the lipid degradation, lipase and esterase lipase, which appeared not related to TOC content and, thus, to SOM accumulation. Lipase showed the highest activity in Elu and Wh, and was low in Ls. As reported in a previous study (Eichlerova et al., 2015), fungal groups have different patterns of enzymes such as esterase, lipase, α-mannosidase, and α-fucosidase, so that the decrease of both F/B and G+/G- ratios in Ls may justify the variations of soil biochemical activity. Furthermore, it has been shown that a reduction in enzyme activity can occur when arbuscular mycorrhizal fungi (AMF) attach to lignin-derived material such as lignin-derived biochar (Khan et al., 2020). The different enzyme activities among soil layers may also indicate the presence of different microbial metabolic pathway as consequence of selective sorption of aromatic and hydrophobic compounds such as lipids onto clay mineral surfaces, so becoming less available to microbial attack (Kaiser and Guggenberger, 2000). This was most possible in the Ls layer, where clay accumulated. In addition, the lowest activities of α-fucosidase and α-mannosidase in Ls suggested the occurrence of a specific inhibition of these enzymes by clay, as suggested by the high negative correlation coefficient between these enzyme activities and clay content (Table 6).

5. Conclusions

Our findings showed that, in mountain soils developed from calcareous parent materials, pedogenic processes such as mineral weathering and lessivage affect the soil biochemical properties along the solum. The mineral fraction stabilized SOM in Tp and Ls, where the organo-mineral interactions were more effective through the involvement of minerals like smectite and iron oxides in Tp and illuviated clays in Ls. In Wh, where both organic substrates and enzymes were adsorbed onto clay minerals, the microbial functions related to SOM degradation were more conservative, contributing to the incipient phase of carbon sequestration in the horizons forming this layer. In this layer, the microbial community was dominated by fungi, which were probably responsible for a higher activity of the enzymes involved in the lipid degradation, particularly lipase and esterase lipase. Therefore, soil functionality, expressed by microbial community and enzyme activities, varies following weathering and lessivage processes, which differently affect the occurrence of organo-mineral interactions along the soil profile. The lessivage, responsible for the formation of Bt horizons, appeared to be a relevant process able to affect the activities of microbial biomass and enzymes involved in SOM degradation.

Our results advocate that soil forming processes are key to understand the functioning of microbial biomass and enzyme activities involved in SOM decomposition. Further, the used approach, which considers the biochemical properties in relation to the pedogenic processes, can allow the transferability of the results to other environments with similar factors of soil formation.

Funding: This research was supported by the "Departments of Excellence-2018" Program (Dipartimenti di Eccellenza) of the Italian Ministry of Education, University and Research, DIBAF Department of the University of Tuscia, Project "Landscape 4.0—food, wellbeing and environment", and by funds of the Università Politecnica delle Marche.

Bibliography

403 Adams, J.L., Tipping, E., Thacker, S.A., Quinton, J.N., 2018. An investigation of the distribution of
404 phosphorus between free and mineral associated soil organic matter, using density fractionation.
405 Plant Soil 427, 139–148. https://doi.org/10.1007/s11104-017-3478-4
406 Agnelli, A., Celi, L., Corti, G., Condello, L., 2008. Organic matter stabilization in soil aggregates
407 and rock fragments as revealed by low-temperature ashing (LTA) oxidation. Soil Biol. Biochem.
408 40, 1379–1389. https://doi.org/10.1016/j.soilbio.2007.12.008
409 Agnelli, A., Massaccesi, L., De Feudis, M., Cocco, S., Courchesne, F., Corti, G., 2016. Holm oak
410 (*Quercus ilex* L.) rhizosphere affects limestone-derived soil under a multi-centennial forest. Plant
411 Soil 400, 297–314. https://doi.org/10.1007/s11104-015-2732-x .
412 Anderson, H.A., Berrow, M.L., Farmer, V.C., Hepburn, A., Russel, J.D., Walker, A.D., 1982. A
413 reassessment of podzol processes. Eur. J. of Soil Sci. 33, 125–
414 136. https://doi.org/10.1111/j.1365-2389.1982.tb01753.x
415 Asaf Khan, M., Rahman, M., Adnan Ramzani, P.M., Zubair, M., Rasool, B., Kamran Khan, M.,
416 Ahmed, A., Ali Khan, S., Turan, V., Iqbal, M., 2020. Associative effects of lignin-derived
417 biochar and arbuscular mycorrhizal fungi applied to soil polluted from Pb-acid batteries effluents
418 on barley grain safety. Sci. Tot. Environ. 710, 136294
419 https://doi.org/10.1016/j.scitotenv.2019.136294
420 Barré, P., Fernandez-Ugalde, O., Virto, I., Velde, B., Chenu, C., 2014. Impact of phyllosilicate
421 mineralogy on organic carbon stabilization in soils: incomplete knowledge and exciting
422 prospects. Geoderma 235–236: 382–395. http://dx.doi.org/10.1016/j.geoderma.2014.07.029
423 Benitez, E., Melgar, R., Nogales, R., 2004. Estimating soil resilience to a toxic organic waste by
424 measuring enzyme activities. Soil Biol. Biochem. 36 (10), 1615-1623.Bertola S., Cusinato A.,
425 2004. Le risorse litiche dell'Altopiano di Folgaria e il loro utilizzo a Riparo Cogola. Studi Trent.
426 Sci. Nat., Preistoria Alpina, 40, 107–123. ISSN 0393-0157.
427 Bilen, S., Bilen, M., Turan, V., 2019. Relationships between Cement Dust Emissions and Soil
428 Properties. Pol. J. Environ. Stud. 28 (5), 3089-3098.

Boča, A., Van Miegroet, H., 2017. Can carbon fluxes explain differences in soil organic carbon storage under aspen and conifer forest overstories? Forests 8, 118. https://doi.org/10.3390/f8040118

Bockheim, J.G., Gennadiyev, A.N., 2000. The role of soil-forming processes in the definition of taxa in soil taxonomy and the world soil reference base. Geoderma 95, 53–72. https://doi.org/10.1016/S0016-7061(99)00083-X

Boerner, R.E.J., Brinkman, J.A., Smith, A., 2005. Seasonal variations in enzyme activity and organic carbon in soil of a burned and unburned hardwood forest. Soil Biol. Biochem. 37, 1419–1426.

Bonifacio, E., Falsone, G., Simonov, G., Sokolova, T., Tolpeshta, I., 2009. Pedogenic processes and clay transformations in bisequal soils of the Southern Taiga zone. Geoderma 149, 66–75. https://doi.org/10.1016/j.geoderma.2008.11.022

Briendley, G.W., Brown, G., 1980. Crystal structure of clay minerals and their X-ray identification. Mineralogical Society Monograph n.9. London, UK. ISBN-10 : 0903056089

Bruun, T.B., Elberling, B., Christensen, B.T., 2010. Lability of soil organic carbon in tropical soils with different clay minerals. Soil Biol. Biochem. 42, 888–895. https://doi.org/10.1016/j.soilbio.2010.01.009

Burns, R.G., DeForest, J.L., Marxsen, J., Sinsabaugh, R.L., Stromberger, M.E., Wallenstein, M.D., Weintraub, M.N., Zoppini, A., 2013. Soil enzymes in a changing environment: current knowledge and future directions. Soil Biol. Biochem. 58, 216–234. https://doi.org/10.1016/j.soilbio.2012.11.009

Cardelli, V., De Feudis, M., Fornasier, F., Massaccesi, L., Cocco, S., Agnelli, A., Weindorf, D.C., Corti, G., 2019. Changes of topsoil under *Fagus sylvatica* along a small latitudinal-altitudinal gradient. Geoderma 344 164–178. https://doi.org/10.1016/j.geoderma.2019.01.043

Chadwick, O. A., Derry, L. A.,Vitousek, P. M., Huebert, B. J. Hedin, L. O., 1999. Changing sources of nutrients during four million years of ecosystem development. Nature 397, 491–497.

455 Chenu, C., Le Bissonnais, Y., Arrouays, D., 2000. Organic matter influence on clay wettability and
456 soil aggregate stability. Soil Sci. Soc. Am. J. 64, 1479–1486.
457 https://doi.org/10.2136/sssaj2000.6441479x
458 Corti, G., Agnelli, A., Ugolini, F.C. 1997. Release of Al by hydroxy-interlayered vermiculite &
459 hydroxy-interlayered smectite during determination of cation exchange capacity in fine earth and
460 rock fragments fractions. Eur. J. Soil Sci. 48, 249-262. https://doi.org/10.1111/j.1365-
461 2389.1997.tb00545.x
462 Corti, G., Agnelli, A., Cocco, S., Cardelli, V., Masse, J., Courchesne, F., 2019. Soil affects
463 throughfall and stemflow under Turkey oak (*Quercus cerris* L.). Geoderma 333, 43-56.
464 10.1016/j.geoderma.2018.07.010
465 Dahlgren, R.A., Ugolini, F.C., 1989. Formation and stability of imogolite in a tephritic Spodosols,
466 Caascade Range, Washington, U.S.A.. Geochim. Cosmochim. Ac. 53, 1897–1904.
467 https://doi.org/10.1016/0016-7037(89)90311-6
468 De Feudis, M., Cardelli, V., Massaccesi, L., Bol, R., Willbold, S., Cocco, S., Corti, G., Agnelli, A.,
469 2016. Effect of beech (*Fagus sylvatica* L.) rhizosphere on phosphorous availability in soils at
470 different altitudes (Central Italy). Geoderma 276, 53–63.
471 https://doi.org/10.1016/j.geoderma.2016.04.028
472 De Feudis, M., Cardelli, V., Massaccesi, L., Hofmann, D., Berns, A.E., Bol, R., Cocco, S., Corti,
473 G., Agnelli, A., 2017a. Altitude affects the quality of the water-extractable organic matter
474 (WEOM) from rhizosphere and bulk soil in European beech forests. Geoderma 302, 6–13.
475 https://doi.org/10.1016/j.geoderma.2017.04.015
476 De Feudis, M., Cardelli, V., Massaccesi, L., Lagomarsino, A., Fornasier, F., Westphalen, D.J.,
477 Cocco, S., Corti, G., Agnelli, A., 2017b. Influence of altitude on biochemical properties of
478 European Beech (*Fagus sylvatica* L.) forest soils. Forests 8, 1–14.
479 https://doi.org/10.3390/f8060213

De Feudis, M., Cardelli, V., Massaccesi, L., Trumbore, S.E., Vittori Antisari, L., Cocco, S., Corti, G., Agnelli, A., 2019. Small altitudinal change and rhizosphere affect the SOM light fractions but not the heavy fraction in European beech forest soil. Catena 181, 104091. https://doi.org/10.1016/j.catena.2019.104091

Dixon, J.B., Schulze, D.G., 2002. Soil Mineralogy With Environmental Applications. SSSA Book Series, 7, Soil Science Society of America, Madison, WI. ISBN 0891188398

Egli, M., Mirabella, A., Sartori, G., Fitze, P., 2003. Weathering rates as a function of climate: results from a climosequence of the Val Genova (Trentino, Italian Alps). Geoderma 111, 99–121. https://doi.org/10.1016/S0016-7061(02)00256-2

Eichlerová, I., Homolka, L., Žifčáková, L., Ludmila, L., Dobiášová, P., Baldrian, P., 2015. Enzymatic systems involved in decomposition reflects the ecology and taxonomy of saprotrophic fungi. Fungal Ecol. 13, 10–22. https://doi.org/10.1016/j.funeco.2014.08.002

Eusterhues, K., Rumpel C., Kleber, M., Kögel-Knabner, I., 2003. Stabilization of soil organic matter by interactions with minerals as revealed by mineral dissolution and oxidative degradation. Org. Geochem. 34, 1591–1600. https://doi.org/10.1016/j.orggeochem.2003.08.007

Fanin, N., Kardol, P., Farrell, M., Nilsson, M.C., Gundale, M.J., Wardle, D.A., 2019. The ratio of Gram- positive to Gram- negative bacterial PLFA markers as an indicator of carbon availability in organic soils. Soil Biol. Biochem. 128, 111–114. https://doi.org/10.1016/j.soilbio.2018.10.010

Fierer, N., Schimel. J.P., Holden. P.A., 2003.Variations in microbial community composition through two soil depth profiles. Soil Biol. Biochem. 35, 167–176. https://doi.org/10.1016/S0038-0717(02)00251-1

Gartzia-Bengoetxea, N., Virto, I., Arias-Gonzalez, A., Enriqu A., Fernandez-Ugalde, O., Barre, P., 2020. Mineral control of organic carbon storage in acid temperate forest soils in the Basque Country. Geoderma 358, 113998. https://doi.org/10.1016/j.geoderma.2019.113998

Gee, G.W., Bauder, J.W., 1986. Particle-size analysis, In: Klute, A. (Ed.), Methods of Soil Analysis, Part 1, Second edition. Agronomy, 9. ASA and SSSA, Madison WI, USA, pp. 383–411. https://doi.org/10.2136/sssabookser5.1.2ed.c15

Houfani, A.A., Větrovský, T., Navarrete, O.U., Štursová, M., Tláskal, V., Beiko, R.G., Boucherba, N., Baldrian, P., Benallaoua, S., Jorquera, M.A., 2019. Cellulase−Hemicellulase Activities and Bacterial Community Composition of Different Soils from Algerian Ecosystems. Microb. Ecol. 77, 713–725. https://doi.org/10.1007/s00248-018-1251-8

ISPRA 2010. Note illustrative della Carta Geologica d'Italia alla scala 1:50.000, Foglio 060, Trento. Servizio Geologico d'Italia, Roma.

Kaiser, K., Guggenberger, G., 2000. The role of DOM sorption to mineral surfaces in the preservation of organic matter in soils. Org. Geochem. 31, 711–725. https://doi.org/10.1016/S0146-6380(00)00046-2

Kaplan, D.I., Bertsch, P., Adriano, D.C., 1997. Mineralogical and physicochemical differences between mobile and nonmobile colloidal phases in reconstructed pedons. Soil Sci. Soc. Am. J. 61, 641–649. https://doi.org/10.2136/sssaj1997.03615995006100020038x

Kögel-Knabner, I., Guggenberger, G., Kleber, M., Kandeler, E., Kalbitz, K., Scheu, S., Eusterhues, K., Leinweber, P., 2008. Organo-mineral associations in temperate soils: Integrating biology, mineralogy, and organic matter chemistry. J. Plant NutSoil Sci. 171, 61–82. https://doi.org/10.1002/jpln.200700048

Lavkulich, L.M.,Wiens, J.H., 1970. Comparison of organic matter destruction by hydrogen peroxide and sodium hypochlorite and its effect on selected mineral constituents. Soil Sci. Soc. Am. Proc. 34, 755–758.

Le Bissonnais, Y., Arrouays, D., 1997. Aggregate stability and assessment of soil crustability and erodibility: II. Application to humic loamy soils with various organic carbon contents. Eur. J. Soil Sci. 48, 39–48. https://doi.org/10.1111/j.1365-2389.1997.tb00183.x

529 Legros, J.P., 1992. Soils of Alpine mountains. In: Martini I.P., Chesworth W. (eds), Weathering
530 soils and paleosoils. Developments in earth surface processes, n. 2. Elsevier, Amsterdam, pp 55–
531 181. ISBN: 9781483291277
532 Levy, G.J., Eisenberg, H., Shainberg, I., 1993. Clay dispersion as related to soil properties and
533 water permeability. Soil Sci. 155(1), 15–22.
534 Likens, G.E., Driscoll, C.T., Buso, D.C., Mitchell, M.J., Lovett, G.M., Bailey, S.W., Siccama, T.G.,
535 Reiners, W.A., Alewell, C., 2002. The biogeochemistry of sulfur at Hubbard Brook.
536 Biogeochem. 60, 235–316. https://doi.org/10.1023/A:1020972100496
537 Marinari, S., Moscatelli, M.C., Marabottini, R., Moretti, P., Vingiani, S., 2020. Enzyme activities as
538 affected by mineral properties in buried volcanic soils of southern Italy. Geoderma 362, 114123.
539 https://doi.org/10.1016/j.geoderma.2019.114123
540 Massaccesi, L., Benucci, G.M.N., Gigliotti, G., Cocco, S., Corti, G., Agnelli, A., 2015. Rhizosphere
541 effect of three plant species of environment under periglacial conditions (Majella Massif, central
542 Italy). Soil Biol. Biochem. 89, 184–195. https://doi.org/10.1016/j.soilbio.2015.07.010.
543 Massaccesi, L., De Feudis, M., Leccese, A., Agnelli, A., 2020. Altitude and vegetation affect soil
544 organic carbon, basal respiration and microbial biomass in Apennine forest soils. Forests 11,
545 710. https://doi.org/10.3390/f11060710
546 Mehra, O.P., Jackson, M.L., 1960. Iron oxide removal from soils and clays by a dithionite-citrate
547 system buffered with sodium bicarbonate. Clays and clay minerals. Proceedings of the 7th
548 National Conference on Clays and Clay Minerals. Oct. 20–23, 1958, Washington, D.C., Clay
549 Clay Min. 7, 317-327. http://dx.doi.org/10.1346/CCMN.1958.0070122
550 Mikutta, R., Kleber, M., Torn, M.S., Jahn, R., 2006. Stabilization of Soil Organic Matter:
551 Association with Minerals or Chemical Recalcitrance?. Biogeochem. 77, 25–56.
552 https://doi.org/10.1007/s10533-005-0712-6
553 Mikutta, R., Mikutta, C., Kalbitz, K., Scheel, T., Kaiser, K., Jahn, R., 2007. Biodegradation of
554 forest floor organic matter bound to minerals via different binding mechanisms. Geochim.

555 Cosmochim. Ac. 71, 2569–2590. https://doi.org/10.1016/j.gca.2007.03.002
556 Moscatelli, M.C., Secondi, L., Marabottini, R., Papp, R., Stazi, S.R., Mania, E., Marinari, S., 2018.
557 Assessment of soil microbial functional diversity: land use and soil properties affect CLPP-
558 MicroResp and enzymes responses. Pedobiologia 66, 36-42.
559 https://doi.org/10.1016/j.pedobi.2018.01.001
560 Nannipieri, P., Giagnoni, L., Renella, G., Puglisi, E., Ceccanti, B., Masciandaro, G., Fornasier, F.,
561 Moscatelli, M.C., Marinari, S., 2012. Soil enzymology: classical and molecular approaches. Biol.
562 Fertil. Soils 48, 743–762. https://doi.org/10.1007/s00374-012-0723-0
563 Orsini, L., Rémy, J., 1976. Utilisation du chlorure de cobaltihexamine pour la détermination
564 simultanée de la capacité d'échange et des bases échangeables des sols. B. Assoc. Fr. Etud. Sol.
565 4, 269–279.
566 Presley, D.R., Ransom, M.D., Kluitenberg, G.J., Finnell, P.R., 2004. Effect of thirty years irrigation
567 on the genesis and morphology of two semiarid soils in Kansas. Soil Sci. Soc. Am. J. 68, 1916–
568 1926. https://doi.org/10.2136/sssaj2004.1916
569 Quénard, L., Samouëlian, A., Laroche, B., Cornu, S., 2011. Lessivage as a major process of soil
570 formation: A revisitation of existing data. Geoderma 167-168, 135-147.
571 https://doi.org/10.1016/j.geoderma.2011.07.031
572 Righi, D., Huber, K., Keller, C., 1999. Clay formation and podzol development from postglacial
573 moraines in Switzerland. Clay Min. 34, 319–332. https://doi.org/10.1180/000985599546253
574 Schaetzl, R.J. and Anderson, S., 2005. Soils: Genesis and Geomorphology. Cambridge University
575 Press
576 Schoeneberger, P.J., Wysocki, D.A., Benham, E.C. and Soil Survey Staff, 2012. Field book for
577 describing and sampling soils. Version 3.0. Natural Resources Conservation Service, National
578 Soil Survey Center, Lincoln, NE. ISBN 978-0-16-091542-0
579 Sidari, M., Ronzello, G., Vecchio, G., Muscolo, A., 2008. Influence of slope aspects on soil
580 chemical and biochemical properties in a *Pinus laricio* forest ecosystem of Aspromonte

581 (Southern Italy). European Journal of Soil Biology 44, 364–372
582 https://doi.org/10.1016/j.ejsobi.2008.05.001
583 Singh, M., Sarkar, B., Sarkar, S., Churchman, J., Bolan, N., Mandal, S., Menon, M., Purakayastha,
584 T.J., Beerling, D.J., 2018. Stabilization of Soil Organic Carbon as Influenced by Clay
585 Mineralogy. Adv. Agron. 148, 33–84. https://doi.org/10.1016/bs.agron.2017.11.001
586 Skopp, J., Jawson M.D., Doran, J.W., 1990. Steady-State Aerobic Microbial Activity as a Function
587 of Soil Water Content. Soil Sci. Soc. Am. J. 54, 1619–
588 1625. https://doi.org/10.2136/sssaj1990.03615995005400060018x
589 Soil Survey Staff (2014) Keys to Soil Taxonomy. 12th Edition, USDA-Natural Resources
590 Conservation Service, Washington DC.
591 Sollins, P., Homann, P., Caldwell, B.A. 1996. Stabilization and destabilization of soil organic
592 matter: mechanisms and controls. Geoderma, 74 (1–2), 65-105. https://doi.org/10.1016/S0016-
593 7061(96)00036-5
594 Torn M.S., Trumbore S.E., Chadwick O.A., Vitousek P.M. and Hendricks D.M. 1997. Mineral
595 control of soil organic carbon storage and turnover. Nature 389: 170–173.
596 https://doi.org/10.1038/38260
597 Tosoni, D., 2011. Carta geologica dell'Altopiano del Tesino (Provincia di Trento). Coord. Scient.
598 Selli L., Università di Bologna.
599 Trasar-Cepeda, C., Leirós, M.C., Gil-Sotres, F., Gil-Sotres, F., 2008. Hydrolytic enzyme activities
600 in agricultural and forest soils. Some implications for their use as indicators of soil quality. Soil
601 Biol. Biochem. 40(9), 2146-2155. https://doi.org/10.1016/j.soilbio.2008.03.015
602 Turan, V., 2004. Confident performance of chitosan and pistachio shell biochar on reducing Ni
603 bioavailability in soil and plant plus improved the soil enzymatic activities, antioxidant defense
604 system and nutritional quality of lettuce. Ecotox. Environ. Safe. 183, 109594.
605 https://doi.org/10.1016/j.ecoenv.2019.109594

606 Van Breemen, N., Buurman, P., 2002. Soil formation, 2nd edition. Kluwer academic publishers,
607 Dordrecht, The Netherlands. https://doi.org/10.1007/0-306-48163-4
608 Vance, E.D., Brookes, P.C., Jenkinson, D.S., 1987. An extraction method for measuring soil
609 microbial biomass C. Soil Biol. Biochem. 19, 703–707. https://doi.org/10.1016/0038-
610 0717(87)90052-6
611 Vepsalainen A.H., Kukkonen S., Vestberg M., Sirvio H., Niemi R.M., 2001. Application of soil
612 enzymes activity test kit in a field experiment. Soil Biol. Biochem. 33, 1665–1672.
613 https://doi.org/10.1016/S0038-0717(01)00087-6
614 Vittori Antisari, L., Bianchini, G., Dinelli, E., Falsone, G., Gardini, A., Simoni, A., Tassinari, R.,
615 Vianello, G., 2014. Critical evaluation of an intercalibration project focused on the definition of
616 new multi-element soil reference materials (AMS-MO1 and AMS-ML1). EQA – International.
617 Journal of Environmental Quality 15, 41–64. https://doi.org/10.6092/issn.2281-4485/4553
618 Vittori Antisari, L., Laudicina, V.A., Falsone, G., Carbone, S., Badalucco, L., Vianello, G., 2016.
619 Native and planted forest species determine different carbon and nitrogen pools in Arenosol
620 developed on Holocene deposits from a costal Mediterranean area (Tuscany, Italy). Environ.
621 Earth Sci. 75, 776. https://doi.org/10.1007/s12665-016-5581-x
622 Vittori Antisari, L., Agnelli, A., Corti, G., Falsone, G., Ferronato, C., Marinari, S., Vianello, G.,
623 2018. Modern and ancient pedogenesis as revealed by Holocene fire - Northern Apennines,
624 Italy. Quatern. Int. 467B, 264-276. https://doi.org/10.1016/j.quaint.2017.12.050
625 Wang, T., Tian, Z., Bengtson, P., Tunlid, A., Persson, P., 2017. Mineral surface-reactive
626 metabolites secreted during fungal decomposition contribute to the formation of soil organic
627 matter. Environ Microbiol, 19, 5117-5129. https://doi.org/10.1111/1462-2920.13990
628 Wiseman C.L.S. and Pu¨ ttmann W. 2005. Soil organic carbon and its sorptive preservation in
629 central Germany. Eur. J. Soil Sci. 56: 65–76. https://doi.org/10.1111/j.1351-0754.2004.00655.x
630 Worrall, F., Parker, A., Rae, J.E., Johnson, A.C., 1999. A study of suspended and colloidal matter in
631 the leachate from lysimeters and its role in pesticide transport. Journal of Environmental Quality

28, 595–604. https://doi.org/10.2134/jeq1999.00472425002800020025x

Zelles, L., 1999. Fatty acid patterns of phospholipids and lipopolysaccharides in the characterisation of microbial communities in soil: a review. Biol. Fertil. Soils, 29, 111–129. https://doi.org/10.1007/s003740050533

Table 1. Values of pH, total organic C (TOC), total N (TN), extractable C (C_{extr}), C_{extr}/TOC ratio, total P (P_T), and total S (S_T) for the investigated soil layers. Values within brackets represent the standard errors. Different letter indicates significant difference among soil layers ($p<0.05$). Brocon Pass, north-eastern Italian Alps.

Soil layers	*n*	pH	TOC	TN	C_{extr}	C_{extr}/TOC	P_T	S_T
			g kg^{-1}	g kg^{-1}	mg kg^{-1}	%	mg kg^{-1}	mg kg^{-1}
Tp	*8*	4.82 b	83.5 a	9.67 a	1328 a	1.80 b	1282 a	700 a
		(0.21)	(15.4)	(1.71)	(177)	(0.26)	(192)	(157)
Elu	*4*	4.55 b	49.9 ab	5.28 a	1188 a	2.62 ab	1197 a	644 a
		(0.05)	(12.5)	(1.30)	(220)	(0.56)	(69)	(79)
Wh	*9*	4.80 b	24.9 b	2.81 b	738 b	3.43 a	749 b	299 b
		(0.16)	(5.4)	(0.61)	(96)	(0.46)	(101)	(56)
Ls	*9*	5.97 a	27.6 b	2.42 b	524 c	3.27 a	767 b	262 b
		(0.38)	(13.0)	(0.63)	(83)	(0.61)	(85)	(45)

n: number of replicates for each layer.
C_{extr}: C extracted by 0.5 M K_2SO_4 solution .

Table 2. Concentrations of pseudo-total elements (Al_T, Fe_T, Ca_T, K_T, Mg_T, Mn_T, and Na_T), clay, Fe and Al extracted by DCB (Fe_{DCB}, Al_{DCB}), cation exchange capacity (eCEC), base saturation (BS), and electrical conductivity (EC) in the investigated soil layers. Values within brackets represent the standard errors. Different letter indicates significant difference among soil layers ($p<0.05$). Brocon Pass, north-eastern Italian Alps.

Soil layers	*n*	Al_T	Fe_T	Ca_T	K_T	Mg_T	Mn_T	Na_T	Clay	Fe_{DCB}	Al_{DCB}	eCEC	BS	EC
		g kg^{-1}						mg kg^{-1}	g kg^{-1}			$cmol_+$ kg^{-1}	%	dS m^{-1}
Tp	*8*	52.6 b	29.8 b	2.5 b	10.6 c	7.6 c	2.5 a	502 a	628 b	19.3 ab	4.1 b	30.9 a	54.4 b	0.35 a
		(2.6)	(1.6)	(0.4)	(0.4)	(0.6)	(0.4)	(52)	(39)	(0.7)	(0.3)	(3.3)	(8.6)	(0.08)
Elu	*4*	50.1 b	32.0 ab	1.5 b	9.8 c	6.6 c	1.6 a	494 a	634 b	23.3 a	5.3 a	33.9 a	79.3a	0.09 b
		(1.9)	(2.5)	(0.5)	(0.3)	(0.2)	(0.2)	(24)	(37)	(2.1)	(0.5)	(3.4)	(8.0)	(0.01)
Wh	*9*	60.6 a	35.2 a	2.3 b	11.5 b	9.3 b	2.6 a	487 a	667 ab	20.4 a	5.1 a	29.0 a	56.2 b	0.07 b
		(2.0)	(0.9)	(0.4)	(0.5)	(0.5)	(0.4)	(38)	(26)	(0.5)	(0.2)	(3.2)	(9.1)	(0.02)
Ls	*9*	61.7 a	34.8 a	6.1 a	12.6 a	10.7 a	2.5 a	532 a	692 a	18.4 b	3.4 c	31.1 a	65.8 a	0.20 a
		(1.3)	(0.6)	(1.3)	(0.4)	(0.2)	(0.4)	(29)	(24)	(0.7)	(0.3)	(3.8)	(7.1)	(0.05)

n: number of replicates for each layer.

Table 3. Semi-quantitative mineralogical composition of the investigated soil layers. Values within brackets represent the standard errors. Brocon Pass, north-eastern Italian Alps.

Soil layers	*n.*	Q	P	O	M	S	HIS	Kao
		%						
Tp	*8*	46(5) a	5(1) a	4(1) a	4(1) a	31(1)* b	7(2) a	3(1) a
Elu	*4*	47(2) a	6(2) a	5(1) a	7(1) a	32(1)* b	1(0) b	2(1) a
Wh	*9*	41(2) a	6(2) a	5(0) a	8(1) a	31(1) b	4(1) ab	5(1) a
Ls	*9*	42(2) a	5(2) a	4(1) a	5(1) a	35(1) a	5(0) ab	4(1) a

n: number of replicates for each layer.
Q = quartz, P = plagioclases, O = orthoclase, M = micas, S = smectite, HIS = hydroxy-aluminum interlayered smectite, Kao = kaolinite.
* mainly disordered smectite.

Table 4. Soil microbial biomass C (MBC) and N (MBN), and results of El-FAME analysis for the investigated soil layers. Values within brackets represent the standard errors. Different letter indicates significant difference among soil layers ($p<0.05$). Brocon Pass, north-eastern Italian Alps.

Soil layers	*n*	MBC	MBN	LMB- El-FAME	B	F	P	Act	G+	G-	F/B	G+/G-
		mg kg^{-1}		nmol g^{-1}							‰	ratio
Tp	*8*	874 a	246 a	464 a	449 a	11.8 a	2.8 a	53.5 a	130.6 a	178.2 a	28.2 b	0.73 b
		(187)	(129)	(20)	(21)	(1.5)	(0.3)	(5.5)	(7.9)	(8.1)	(4.1)	(0.0)
Elu	*4*	445 ab	151 a	63 c	59 c	3.1 b	0.6 b	6.8 c	18.8 b	18.1 c	47.5 a	1.02 a
		(267)	(55)	(14)	(13)	(0.4)	(0.2)	(1.4)	(4.9)	(4.2)	(3.9)	(0.1)
Wh	*9*	118 b	45 c	120 b	116 b	3.6 b	1.0 b	17.2 b	31.1 b	41.9 b	39.1 a	0.80 b
		(30)	(10)	(37)	(36)	(0.9)	(0.2)	(6.2)	(9.7)	(13.2)	(5.7)	(0.0)
Ls	*9*	227 b	81 b	112 b	109 b	2.3 b	0.4 c	12.8 b	26.8 b	42.4 b	24.4 b	0.69 b
		(102)	(14)	(24)	(23)	(0.4)	(0.0)	(2.8)	(5.6)	(9.3)	(3.5)	(0.0)

n: number of replicates for each layer.

LMB-El-FAME: living microbial biomass determined by El-FAME, B: bacteria, F: saprophytic fungi, P: protozoa, Act: actinomycetes, G+: Gram positive bacteria, G-: Gram negative bacteria, F/B: fungi/bacteria ratio, G+/G-: Gram positive bacteria/Gram negative bacteria ratio.

Table 5. Enzyme activities in the investigated soil layers. Values within brackets represent the standard errors. Different letter indicates significant difference among soil layers ($p<0.05$). Brocon Pass, north-eastern Italian Alps.

Soil layers	*n*	Cell	Chit	BG	AG	AP	Sulph	Xylo	But	a-Gal
		nmol MUF g^{-1} h^{-1}								
Tp	*8*	76.3 a	304 a	389 a	79 a	1506 a	900 a	189 a	1553 a	128 a
		(20.3)	(70)	(98)	(16)	(293)	(166)	(47)	(301)	(29)
Elu	*4*	22.8 b	113 b	142 b	40 b	1034 a	704 a	91 ab	1204 a	100 a
		(7.9)	(33)	(48)	(14)	(282)	(233)	(30)	(299)	(35)
Wh	*9*	19.8 b	105 b	126 b	37 b	571 b	369 b	58 b	880 b	46 b
		(5.1)	(25)	(28)	(9)	(114)	(107)	(21)	(201)	(11)
Ls	*9*	12.2 b	78 b	69 c	17 b	292 c	193 b	23 c	474 c	19 c
		(3.1)	(28)	(16)	(4)	(45)	(59)	(8)	(107)	(4)

Soil layers	*n*	b-Gal	b-Gluc	E-Lip	Lip	LeuAryl	ValAryl	SEI	SEI/MBC
		nmol MUF g^{-1} h^{-1}				nmol AMC g^{-1} h^{-1}	nmol AMC g^{-1} h^{-1}	nmol MUF/AMC g^{-1} h^{-1}	nmol MUF mg^{-1} MBC h^{-1}
Tp	*8*	89 a	203 a	254 a	154 b	132 a	26 a	6067 a	7.9 b
		(25)	(29)	(104)	(30)	(18)	(5)	(1054)	(1.8)
Elu	*4*	64 ab	114 b	301 a	300 a	160 a	22 a	4515 ab	16.5 b
		(22)	(22)	(37)	(108)	(19)	(2)	(1178)	(5.0)
Wh	*9*	37 b	126 b	271 a	359 a	61 b	17 a	3151 b	32.5 a
		(7)	(15)	(54)	(79)	(12)	(2)	(507)	(5.9)
Ls	*9*	18 c	82 c	192 a	198 b	51 b	18 a	1755 c	27.1 ab
		(4)	(14)	(42)	(52)	(11)	(2)	(279)	(10.7)

n: number of replicates for each layer.

Cell: β-cellobiohydrolase; Chit: N-acetyl-ß-glucosaminidase; BG: β-glucosidase; AG: α-glucosidase; AP: Acid phosphomonoesterase; Sulph: arylsulphatase; Xylo: xylosidase; But: butyrate esterase; a-Gal: α-galactosidase; b-Gal: β-galactosidase; b-Gluc: β-glucuronidase; E-Lip: esterase lipase; Lip: Lipase; LeuAm: leucine arylamidase; ValAryl: valine arylamidase; SEI: Synthetic Enzymatic Index; SEI/MBC: Synthetic Enzymatic Index per unit of microbial biomass carbon.

Table 6. Spearman correlation coefficient between physicochemical and biochemical properties for the investigated soil horizons (n=29). Brocon Pass, north-eastern Italian Alps.

	pH	TOC	Total N	C_{ext}/TOC	Clay	EC	Fe_{DCB}/Fe_T	$(Ca_T+Mg_T+K_T+Na_T)/(Al_T+Fe_T$
MBC	-0.399 *	0.643***	0.704***	-0.521 **			0.467*	
MBN		0.589**	0.541**	-0.462 *			0.318 ns	
Cell		0.851***	0.903***	-0.736***			0.572 **	
Chit		0.727***	0.815***	-0.696***			0.510 **	
BG		0.825***	0.884***	-0.656***			0.586 **	
AG		0.781***	0.833***	-0.630***			0.552 **	
AP	-0.501 **	0.836***	0.897***	-0.649***	-0.392 *		0.764***	-0.397 *
Sulph		0.830***	0.889***	-0.692***			0.767***	
Xylo	-0.392 *	0.842***	0.902***	-0.674***			0.704***	
But	-0.489 **	0.814***	0.853***	-0.634 ***	-0.398 *		0.738***	-0.441 *
a-Gal	-0.581 **	0.737***	0.782***	-0.572 **	-0.456 *		0.672***	-0.541 **
b-Gal	-0.563**	0.761***	0.811***	-0.607 **	-0.461 *		0.694	-0.474 **
b-Gluc	-0.501**	0.682***	0.736***	-0.615 **			0.559 **	
a-Man	-0.658***	0.589**	0.608***	-0.423 *	-0.512 **		0.654***	-0.656***
a-Fuc	-0.636***	0.510**	0.515**	-0.394 *	-0.563 **		0.659***	-0.707***
E-Lip								
Lip						-0.464*		-0.480 **
LeuAryl	-0.440 *	0.629***	0.702***	-0.530 **			0.772***	-0.376 *
ValAryl		0.579**	0.616**	-0.593 **			0.606***	
SEI	-0.535 **	0.794***	0.858***	-0.622***	-0.428 *		0.753***	-0.419 *
SEI/TOC	-0.433 *	-0.428*	-0.366 *	0.395 *		-0.711***		
SEI/MBC		-0.515 **	-0.561**	0.435 *				

*** p<0.001; **p<0.01; *p<0.05; TOC: total organic C; C_{extr}/TOC: extractable C/TOC ratio; Fe_{DCB}/Fe_T: Fe extracted by Na-dithionite-citrate-bicarbonate solution/pseudo-total Fe ratio; $(Ca_T+Mg_T+K_T+Na_T)/(Al_T+Fe_T)$: $(Ca_T+Mg_T+K_T+Na_T)/(Al_T+Fe_T)$ molar ratio; MBC and MBN: microbialbiomass C and N, respectively; Cell: β-cellobiohydrolase; Chit: N-acetyl-ß-glucosaminidase; BG: β-glucosidase; AG: α-glucosidase; AP: Acidphosphomonoesterase; Sulph: arylsulphatase; Xylo: xylosidase; But: butyrate esteras; a-Gal: α-galactosidase; b-Gal: β-galactosidase; b-Gluc: β-glucuronidase; a-Man: α-mannosidase; a-Fuc: α-fucosidase; E-Lip: Esterase lipase; Lip: Lipase; LeuAryl: Leucine arylamidase; ValAryl: valine arylamidase; SEI: Synthetic Enzymatic Index; SEI/TOC: Synthetic Enzymatic Index per unit of organic carbon; Synthetic Enzymatic Index per unit of microbial biomass carbon.

FIGURE CAPTIONS

Figure 1. The study area.

Figure 2. Boxplot of Fe_{DCB}/Fe_T ratio, where Fe_{DCB} and Fe_T are amount of Fe extractable with Na-dithionate-citrate-bicarbonate and pseudo-total, respectively (A) and molar ratio between the sum of the Ca_T, Mg_T, K_T, Na_T and Al_T plus Fe_T (B). Different letters mean significant difference at p-level <0.01.

Figure 3. Principal component analysis of the physicochemical properties of soil layers (Tp, Elu, Wh and Ls). On left, plots of first and second components grouping variables, on right table of rotated loading values for the first two PCs from soil samples (in bold significant values p<0.01).

Figure 4. Boxplot of α-mannosidase (A) and α-fucosidase (B) activities. Different letters mean significant difference at p-level <0.05.

Figure 5. Boxplot of lipase activity (A) and Synthetic Enzymatic Index per unit of organic carbon - SEI/OC (B). Different letters mean significant difference at p-level <0.01.

Figure 6. Principal component analysis of the biochemical properties of soil layers (Tp, Elu, Wh, and Ls). On left, plots of first and second components grouping variables, on right table of rotated loading values for the first two PCs from soil samples (in bold significant values p<0.01).

Figure 1

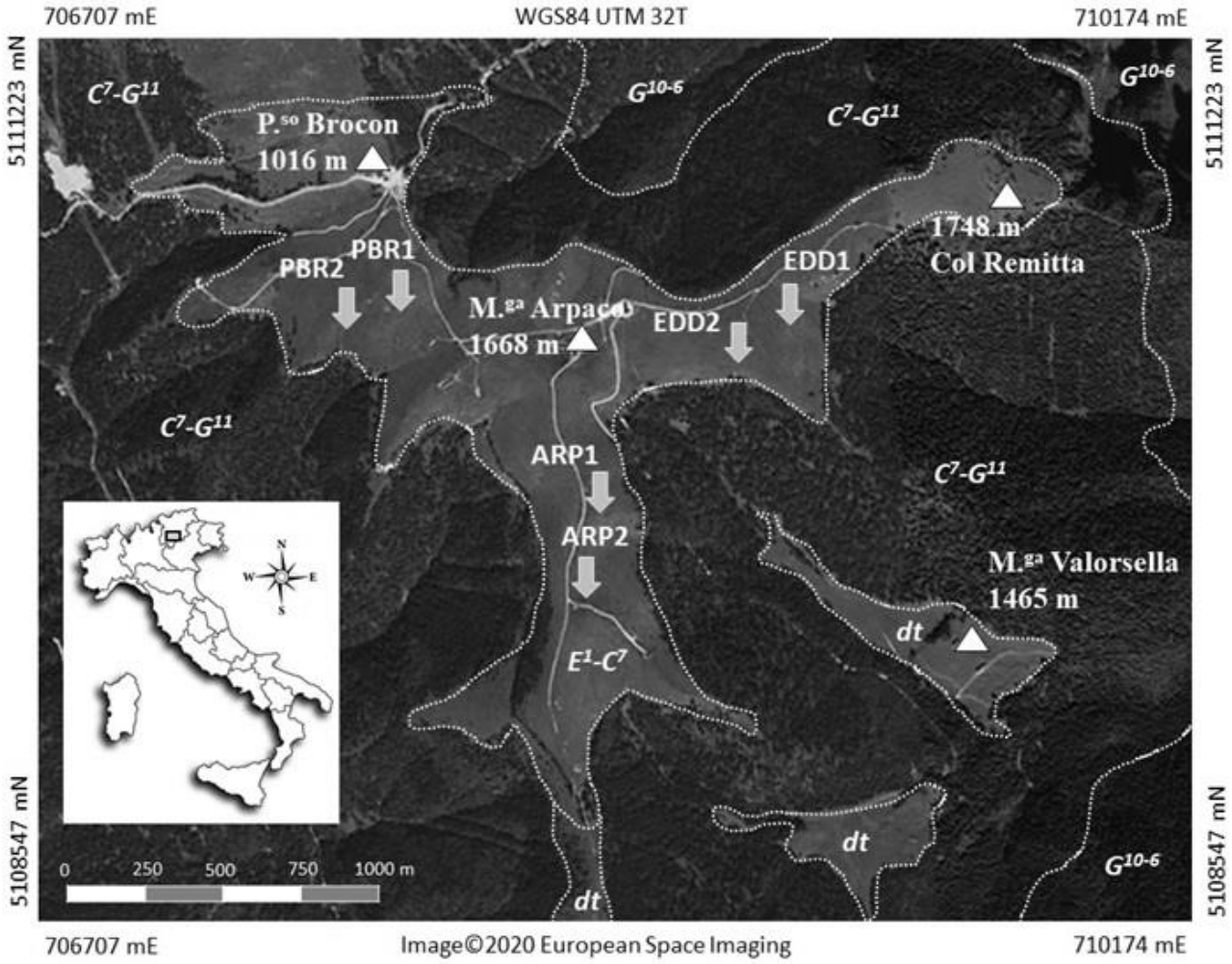

Soil profile location

EDD2

Litological formations in succession from the Upper to Lower Cretaceous

G^{10-6} «Rosso Ammonitico» (Malm-Dogger) White or briek red limestones

C^{7}-G^{11} «Biancone» (Cenomanian-Malm) Greyish – white or white limestones

E^{1}-C^{7} «Scaglia rossa» (Eocene-Cretaceous) Red or pink marls and clayey limestones

dt Heterogeneous glacial debris

Figure 2

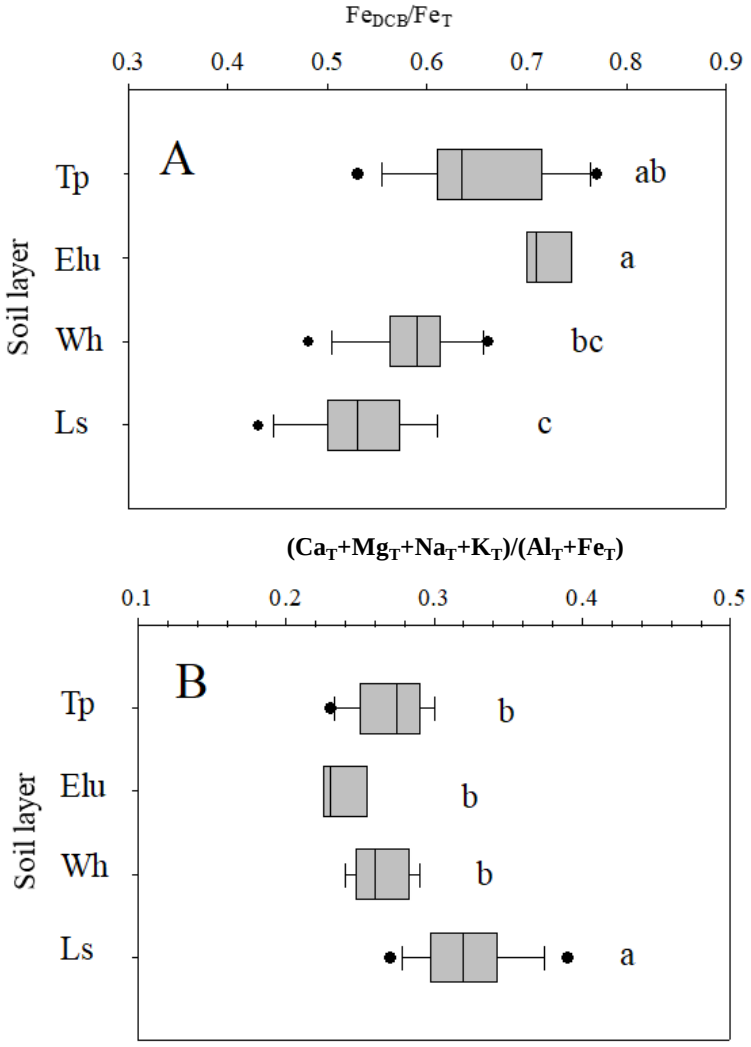
Fe_{DCB}/Fe_T
0.3
0.4
0.5
0.6
0.7
0.8
0.9
A
Tp
Elu
Wh
Ls
Soil layer
ab
a
bc
c
$(Ca_T+Mg_T+Na_T+K_T)/(Al_T+Fe_T)$
0.1
0.2
0.3
0.4
0.5
B
Tp
Elu
Wh
Ls
Soil layer
b
b
b
a

Figure 3

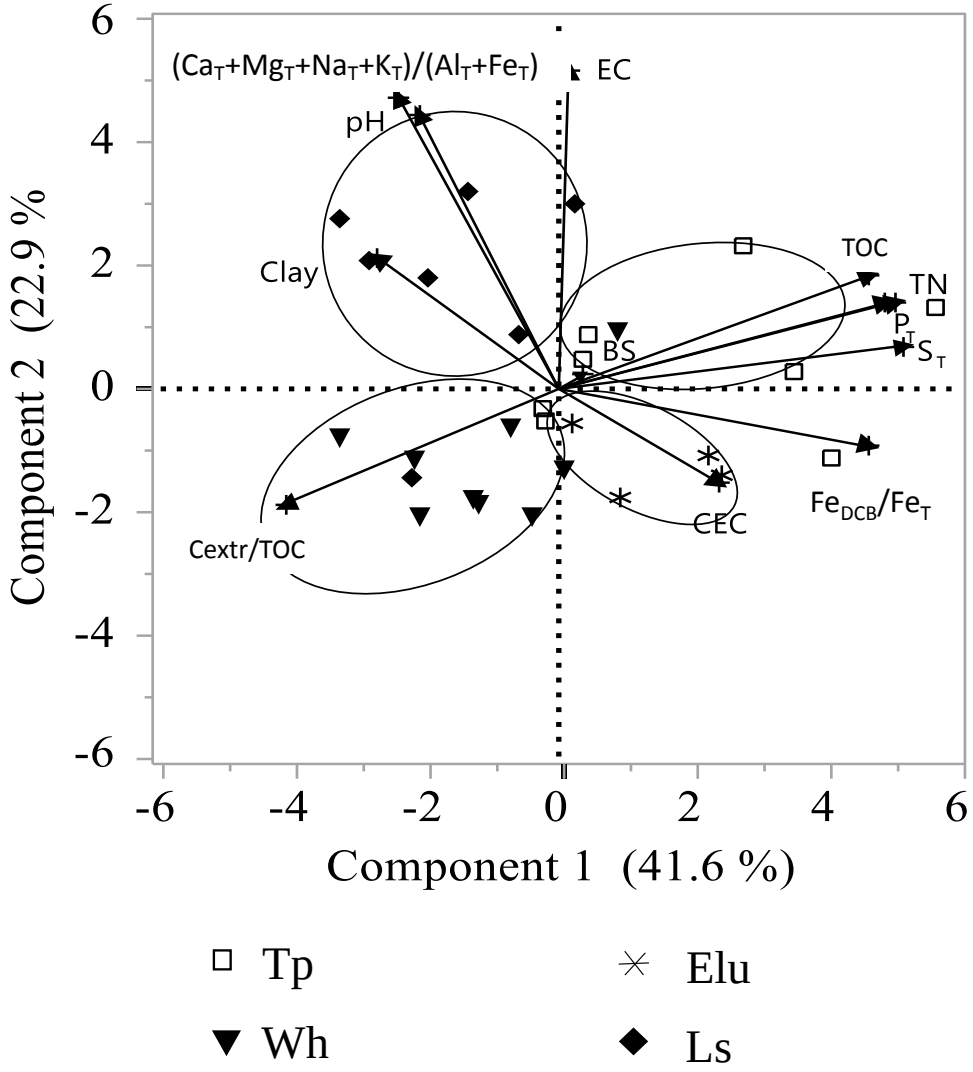

Soil properties	Component 1	Component 2
pH	-0.137	**0.939**
TOC	**0.878**	-0.002
TN	**0.928**	-0.095
C_{extr}/TOC	**-0.735**	-0.060
P_T	**0.870**	-0.048
S_T	**0.880**	-0.179
Clay	-0.325	**0.431**
CEC	0.258	-0.335
BS	0.028	0.026
EC	0.321	**0.847**
Fe_{DCB}/Fe_T	**0.680**	-0.379
$(Ca_T+Mg_T+Na_T+K_T)/(Al_T+Fe_T)$	-0.076	**0.802**
Eigenvalue	4.99	2.74
Accumulated variance	41.6%	**64.5%**

Figure 4

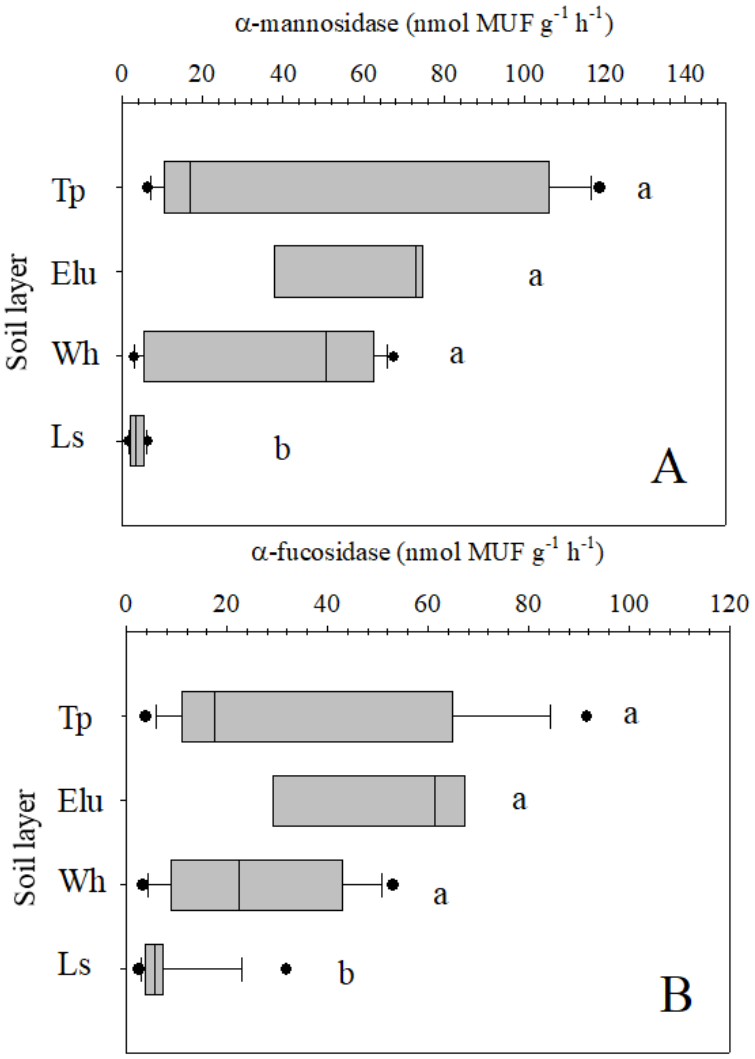
α-mannosidase (nmol MUF g-1 h-1)
0
20
40
60
80
100
120
140
Soil layer
Tp
Elu
Wh
Ls
a
a
a
b
A
α-fucosidase (nmol MUF g-1 h-1)
0
20
40
60
80
100
120
Soil layer
Tp
Elu
Wh
Ls
a
a
a
b
B

Figure 5

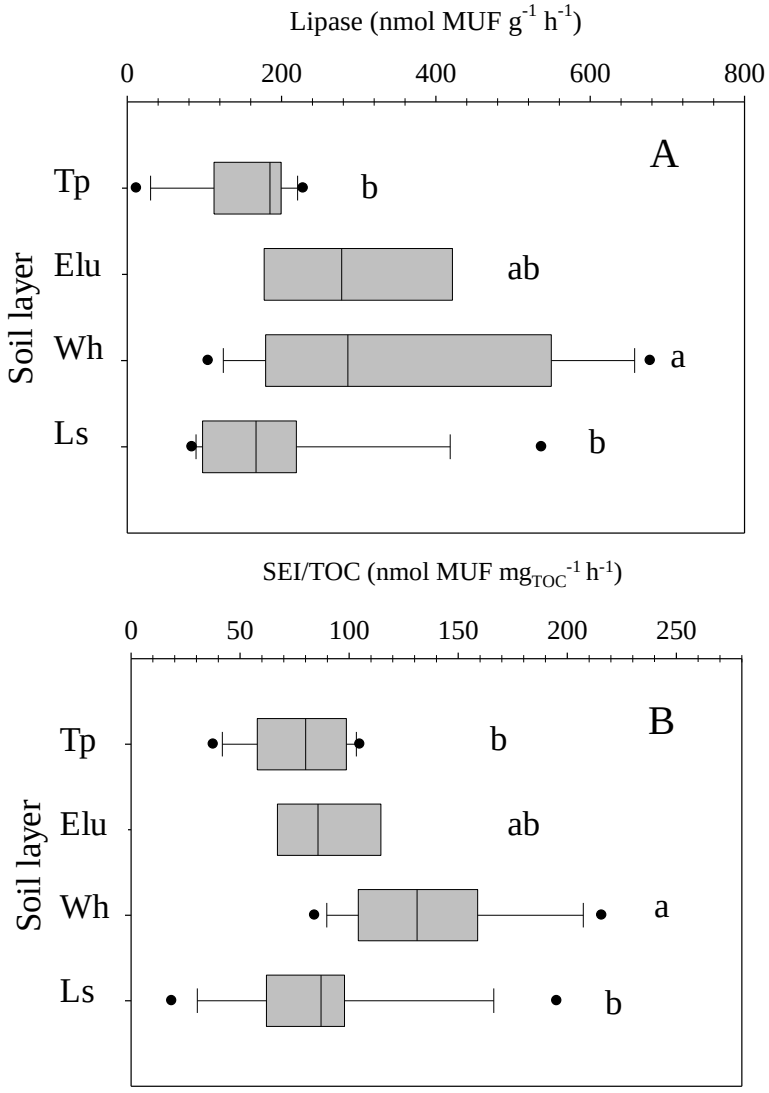
Lipase (nmol MUF g-1 h-1)
0
200
400
600
800
A
Tp
Elu
Wh
Ls
Soil layer
b
ab
a
b
SEI/TOC (nmol MUF mgTOC-1 h-1)
0
50
100
150
200
250
B
Tp
Elu
Wh
Ls
Soil layer
b
ab
a
b

Figure 6

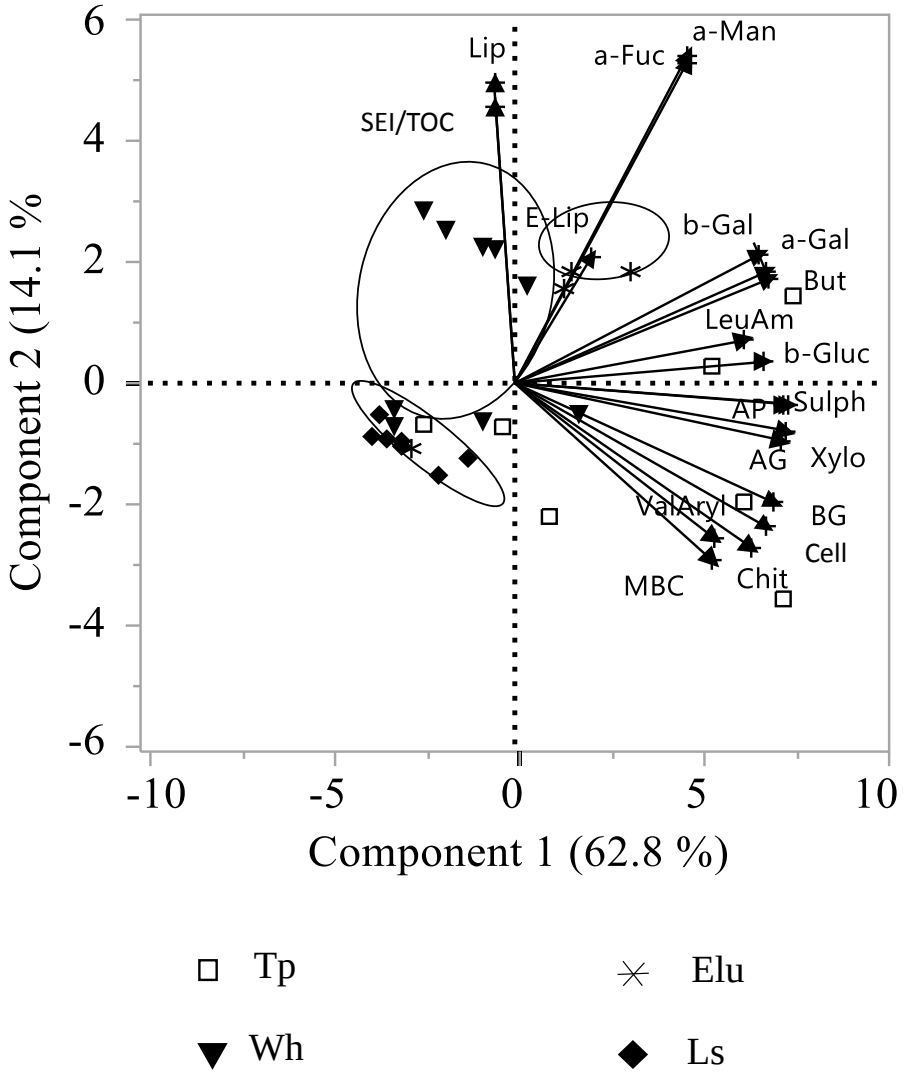

Soil properties	Component 1	Component 2
SEI/TOC	-0.251	**0.555**
MBC	**0.79**	-0.152
Cell	**0.955**	-0.023
Chit	**0.92**	-0.083
BG	**0.966**	0.036
AG	**0.949**	0.174
AP	**0.951**	0.258
Sulph	**0.93**	0.251
Xylo	**0.958**	0.199
But	**0.801**	**0.497**
a-Gal	**0.752**	**0.537**
b-Gal	**0.786**	**0.508**
b-Gluc	**0.833**	0.317
a-Man	0.371	**0.875**
a-Fuc	0.375	**0.859**
E-Lip	0.176	**0.344**
Lip	-0.274	**0.606**
LeuAm	**0.752**	0.339
ValAryl	**0.789**	-0.104
Eigenvalue	11.92	2.68
Accumulated variance	62.8%	**76.9%**

Declaration of interests

xThe authors declare that they have no known competing financial interests or personal relationships that could have appeared to influence the work reported in this paper entitled **MINERAL WEATHERING AND LESSIVAGE AFFECT MICROBIAL COMMUNITY AND ENZYME ACTIVITY IN MOUNTAIN SOILS**

☐The authors declare the following financial interests/personal relationships which may be considered as potential competing interests: